Simulation and Measurement of Beam Halo at ATF2

R. Yang[1], P. Bambade[1], S. Wallon [1], A. Faus-Golfe[1,2],
N. Fuster-Martínez[2], T. Naito[3], A. Aryshev [3], T. Okugi [3]

1. Laboratoire de l'Accélérateur Linéaire (LAL), Orsay, France
2. Instituto de Física Corpuscular(IFIC), Valencia, Spain
3. High Energy Accelerator Research Organization (KEK), Tsukuba, Japan

March 14, 2017

Introduction

What’s Halo? Halo definition

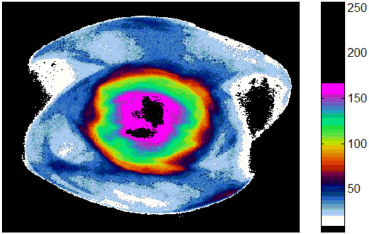

"From the diagnostics point of view, one thing is certainly clear – by definition halo is low density and therefore difficult to measure . . . "
—Halo’03 Workshop

- Regarding the ’non-Gaussian’ component of profile as halo, the ’*Gaussian area ratio*’ is also a quantification of halo

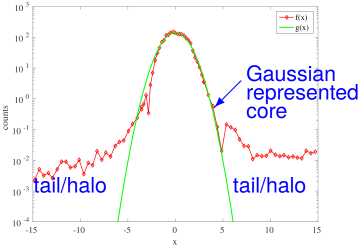

Negative effects:

- Increasing background level; influence precise particle physics experiments (gamma ray & muons from collimator)
- Second beam-beam limit of luminosity of collider

[1] K. Wittenburg, CAS (1992), 557-580
[2] H. Zhang, et al., PRST-AB, 15, 072803 (2012)

Motivation of halo study at ATF2

- Background induced by halo particles loss upstream of IP might reduce the modulation resolution of Shintake monitor
- Purpose to understand the genesis of halo and its distribution at ATF2

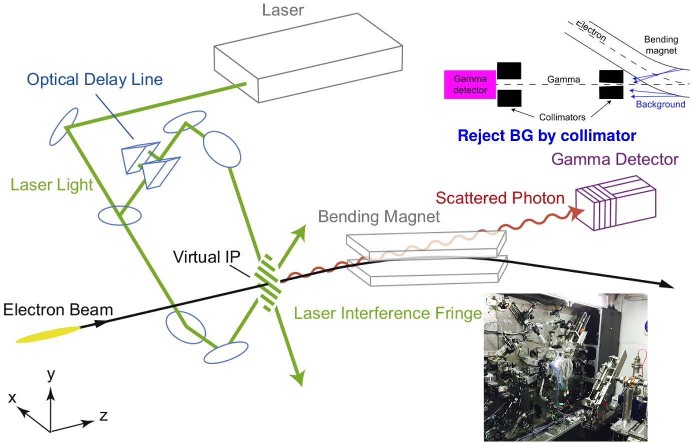

* Figures from [1] J. Yan, et al., NIMA 740(2014) 31-137; [2] T. Suehara, et al., NIMA 616(2010) 1-8

Past and present halo measurement at ATF2

- Diagnostic of beam halo has started since 2005 with wire scanners at ATF EXT line
- New visualization of halo at EXT line and Post-IP of ATF2 were performed using Post-IP WS (2013), YAG screen (2015) and DS (2015)

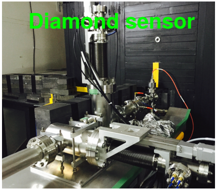

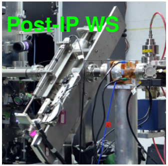

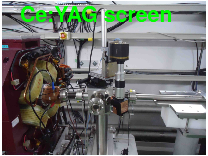

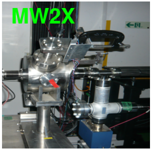

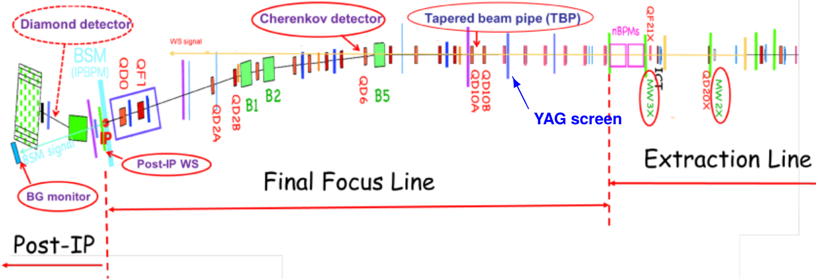

Candidate halo source

- Particles process (beam gas Coulomb scattering, Bremsstrahlung and intra beam scattering), mismatching, field errors,interactions with aperture limits and Potential Well Distortion (PWD)
- Beam halo from BGS at ATF damping ring was first studied by K. Hirata

1D profile prediction

$$\rho(X) = \frac{1}{\pi}\int_0^{\infty} \exp[-\frac{1}{2}k^2 + \frac{N_t}{d}\cdot\frac{2}{\pi}\int_0^1 (\frac{KX\theta_m}{\sigma'_0}\cdot K_1(\frac{KX\theta_m}{\sigma'_0}) - 1)/X\cdot cos^{-1}(X)]dXdK]$$

$$\rho_{tail}(X) \simeq \frac{N_d\beta\theta_{min}}{8\sigma_0 X^3}, (X \to \infty)$$

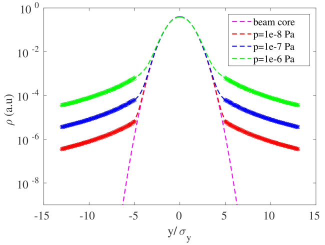

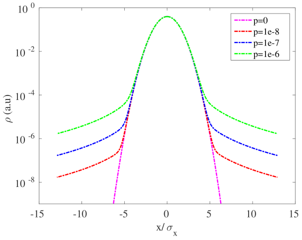

[1] K. Hirata and K. Yokoya, *ParticleAccelerators* 39 (1992), 147-158

Candidate halo source

- Particles process (beam gas Coulomb scattering, Bremsstrahlung and intra beam scattering), mismatching, field errors,interactions with aperture limits and Potential Well Distortion (PWD)
- Beam halo from BGS at ATF damping ring was first studied by K. Hirata

1D profile prediction

$$\rho(X) = \frac{1}{\pi}\int_0^{\infty} \exp[-\frac{1}{2}k^2 + \frac{N_t}{d}\cdot\frac{2}{\pi}\int_0^1 (\frac{KX\theta_m}{\sigma_0'}\cdot K_1(\frac{KX\theta_m}{\sigma_0'}) - 1)/X \cdot cos^{-1}(X)]dXdK]$$

$$\rho_{tail}(X) \simeq \frac{N_d \beta\theta_{min}}{8\sigma_0 X^3}, (X \to \infty)$$

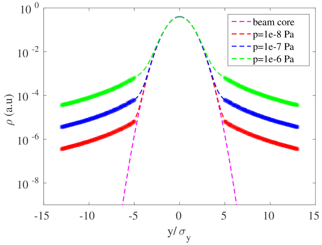

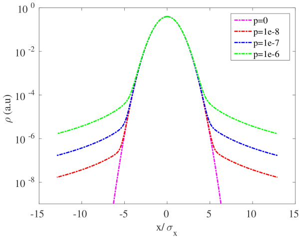

- More detailed and systematic simulation and experiment are essential !

[1] K. Hirata and K. Yokoya, *ParticleAccelerators* 39 (1992), 147-158

Simulation of beam halo from BGS

Equilibrium Emittance

- Setting rotation of quads $\sigma_{\theta q}$ =2 mrad, alignment errors of quads. $\sigma_{dq} = 20\ \mu$m and sext. $\sigma_{ds} = 70\ \mu$m to represent residual coupling and dispersion
- Average of residual η_y is 10∼20 mm
- Equilibrium emittances achieved approximate experimental values

ϵ_x (nm)	ϵ_y (pm)	σ_l (mm)	σ_p (%)	τ_x (ms)	τ_y (ms)	τ_s (ms)
1.2	10∼20	5.3	0.056	20	27.6	21.6

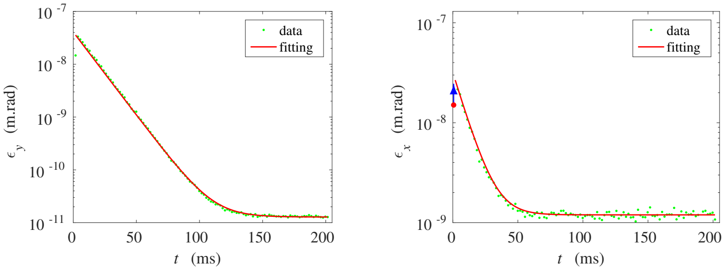

Closed orbit and longitudinal dynamic

- Residual COD and evolution of δp, $\delta z \sim 2\%$ are also considered.
- Mismatching caused by large σ_p of injection is observed ($t < 1$ ms).

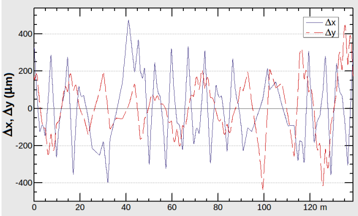

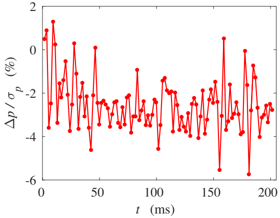

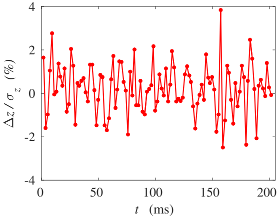

Beam distorsion from alignment errors

- Kurtosis is used to quantify 1D beam profile (for simulation), normalizing to K-V distribution

$$h(x) = \frac{1}{N}\sum_{i=1}^{N}[\frac{x_i - \bar{x}}{\sigma_x}]^4 - \frac{9}{5}$$

- Significant halo when $h > 1.2$, and quite sensitive

	Hollow	Uniform	Gaussian	Gaussian core + flat tail
h	-2/15	0	6/5	11

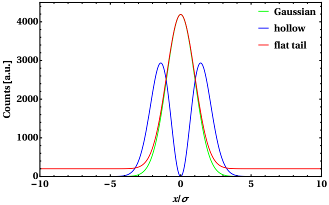

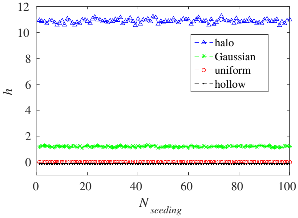

[1] C. Allen, et al., PRST-AB, 2002, 5(12):124202

Beam distorsion from alignment errors

- Tracking of macro-particles (2×10^4) from injection to extraction
- Several seedings of errors are considered, to represent different ϵ_y
- Gaussian transverse beam profiles, and few halo particles, with 20/70 μm alignment errors
- h_x/h_y oscillate around $1.2^{+0.3}_{-0.1}$ along the whole ring (due to η and statistical errors?)

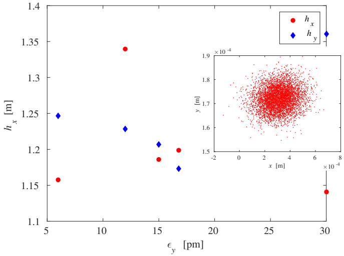

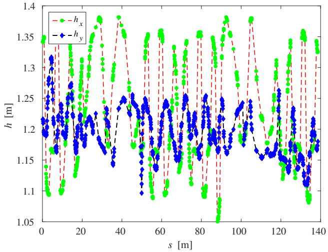

Method of BGS simulation in SAD

- Identify ϵ_x, ϵ_y, σ_z and σ_p at the moment of BGS events happened
- Generate N_j random BGS events in each j-th turn, with varying Twiss parameters according to the position (including multi-BGS)
- Track N_j particles from scattering to common observation point, to be combined with N_{j-1} scattered particles accumulated from previous turns and tracked to observation point
- Repeat the above process until extraction

† Core/BGS particles are tracked separately

† Common beam parameters at injection ($t = 0$)

E (GeV)	$\epsilon_{x,0}$ (nm)	$\epsilon_{y,0}$ (nm)	σ_l (ps)	σ_p	RD/QE
1.282	14	14	15	0.4%	only at Dipoles

Benchmark of BGS simulation

- Benchmarking by vacuum lifetime τ_v prediction, comparing with analytic and measured values
- Elastic BGS and Brems. are considered in simulation
- Simulation parameters:
  E=1.3 GeV, $P = 1 \times 10^{-6}$ Pa, pipe aperture 7.5/12 mm and $\delta_{acc} = 1\%$
- Assuming $\tau^{-1} = \tau_v^{-1} + \tau_{Tou}^{-1}$, and $\tau_v = 1/\alpha P$ is measured by fitting $I(t)$

$$N(t) = N(t_0) - \alpha \int_{t_0}^{t} dt' P(t') N(t') - \frac{1}{\tau_{Tou}}(\kappa) \int_{t_0}^{t} \frac{N^2(t')}{R_{Tou}(N(t'), \kappa)}$$

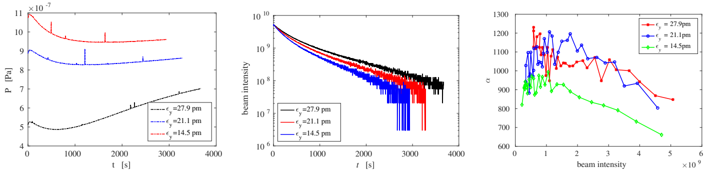

- Vacuum lifetime (1×10^{-6} Pa):
  analytic, 71 mins; simulated, 78 mins;
  measured, 16.6 mins ($\alpha = 1000$ in Jan. 2017)

[1] T. Okugi, et al., NIMA 455(2000) 207-212

Evolution of beam halo with time

- Due to radiation damping, BGS events happened at different moment have different contributions to the final halo distribution
- BGS particles in the last τ_y, $2\tau_y$, $3\tau_y$, $4\tau_y$ are concerned in simulation

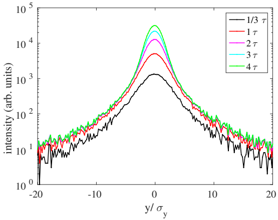

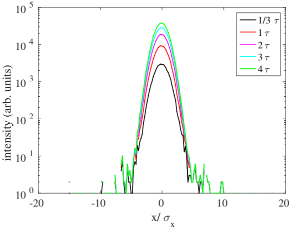

- BGS halo distribution mainly depends on BGS events in the last $2\tau_y$, vertically and horizontally!

Comparison of theoretical/tracking results

- Theoretical estimation is based upon the equilibrium parameters

ϵ_x (nm)	ϵ_y (pm)	$\bar{\beta}_x$ (m)	$\bar{\beta}_y$ (m)	τ_x (ms)	τ_y (ms)	gas
1.2	12.8	4	4.6	20	27.6	CO

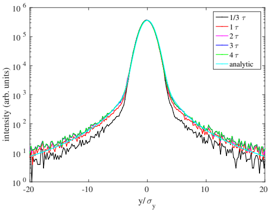

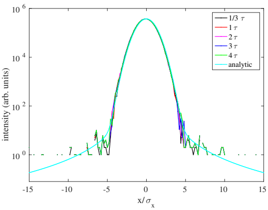

- Halo does reach "equilibrium" for simulation time $t_n > 2\tau_y$
- Vertically, tracking result ($t_n \geq 2\tau_y$) is coincident with the theoretic prediction within $10\sigma_y$, but has higher halo level beyond $10\sigma_y$ (factor 2)
- Horizontally, less beam halo comparing with vertical one, and the quantity ($> 5\sigma_x$) is consistent with theoretic estimation!

Vacuum dependence of beam halo

- Percentage of BGS particles is estimated according to P_{aver} and probability of multi-BGS.
- Vertical beam halo varies according to P_{ave} significantly, while less significant horizontally, due to the statistics

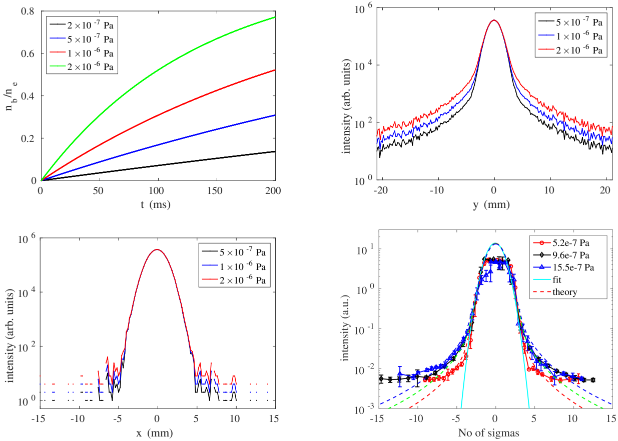

Visualization of beam halo using DS at Post-IP

Halo measurement by *in vacuum* diamond sensor

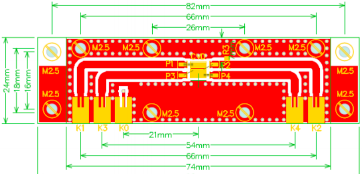

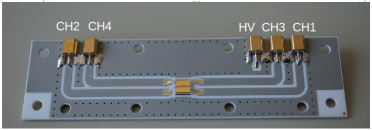

Test of DS

- Leakage current: $\sim$ pA
- Integrated charge by an MIP: 2.88 fC
- Charge collection efficiency: 100 % @ 400 V (small signal)
- Dynamic range $d_R = 10^6$

- Errors: high charge signal reduced by charge collection saturation, and sensitivity limited by induction current
- Reducing d_R and cause profile distortion
- Solutions: carefully alignment, calibration of DS signal and RF-finger/LPFs

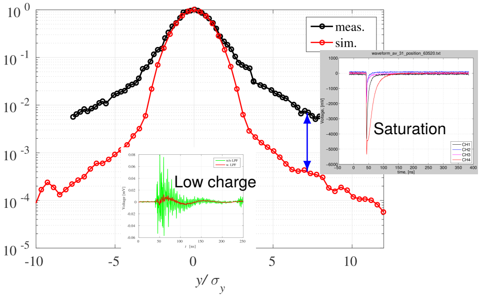

[1] S. Liu, et al., NIMA, 832 (2016)

Recalibration of vertical diamond stripe

- Variating beam intensity and displacing diamond stripe to calibrate readout charge signal with N_e

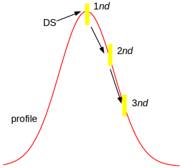

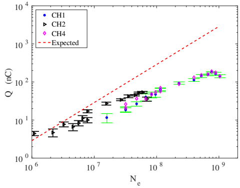

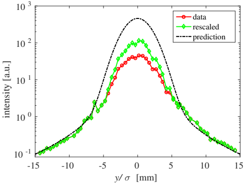

- Saturation start at $N_e \approx 10^7$ and charge collection efficiency reduced to <15% when $N_e > 2 \times 10^8$
- Applying Q_{coll}/Q_{read} to rescale measured profile, and seems closer to expectation

Rescaling based on self-calibration

- Method to rescale data using profile given by broad DS stripe:
  - Fit $\sigma_{x,y}$ from WS data
  - Predict the expected charge Q_{exp} within Gaussian core region, using the charge collection factor given by low charge data
  - Fit $Q_{meas} \propto n_e$ predicted based on beam intensity and $\sigma_{x,y}$
  - Calculate rescaling factor $\kappa(n_e) = Q_{exp}/Q_{meas}$
  - Rescale charge collected within core region using $\kappa(n_e)$

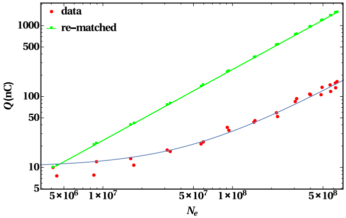

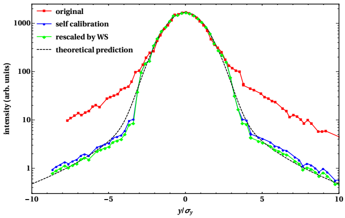

- Beam profile after rescaling is comparable with estimation, while both of them agree well with halo predicted by BGS theory/simulation!

Vacuum dependence of vertical beam halo

- Halo profiles rescaled based on self-calibration, with P_{aver} are $2.3 \times 10^{-7} \sim 1 \times 10^{-6}$ Pa, agree well with BGS theoretic prediction!
- Vertical beam halo is dominated by beam gas Coulomb scattering

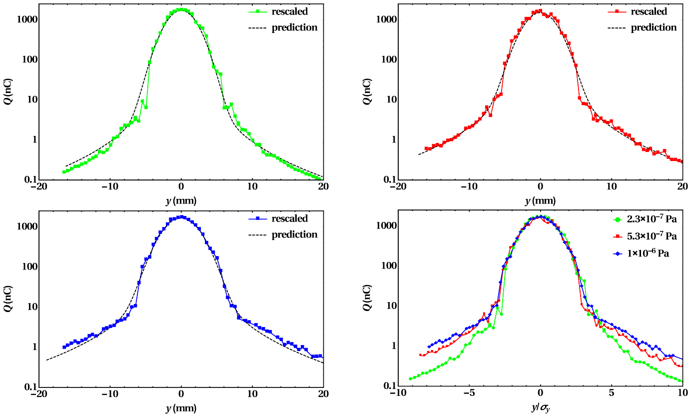

Optimization of horizontal profiles

- Halo measured by DS after rescaling is higher than BGS prediction!
- Asymmetric beam profile is observed, more particles in high energy side

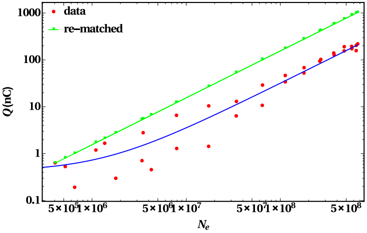

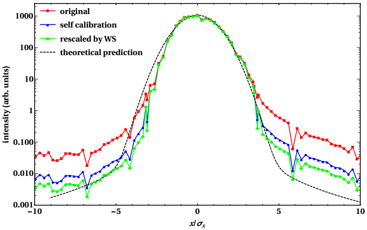

- Reasons: systematic errors of experiment or rescaling, other possible halo source (IBS and PWD?)

Optimization of horizontal profiles

- Halo measured by DS after rescaling is higher than BGS prediction!
- Asymmetric beam profile is observed, more particles in high energy side

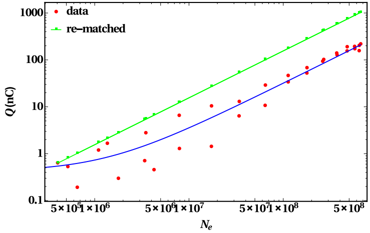

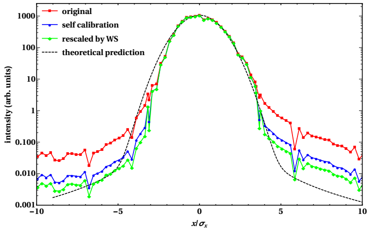

- Reasons: systematic errors of experiment or rescaling, other possible halo source (IBS and PWD?)
- Strategies:
  - Another halo monitor (OTR/YAG screens) at EXT line
  - Simulation of beam distortion due to IBS and PWD

Upgrading of Ce:YAG monitor at EXT line

Present Ce:YAG screen monitor

- Present YAG screen has two separated screens with 1 mm slit and can visualize vertical halo at 0.3 m upstream of QM16

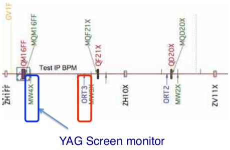

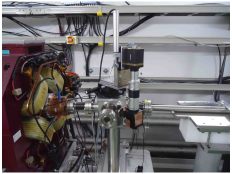

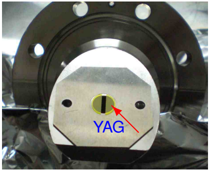

- Dynamic range $d_R < 10^4$, resolution $< 10\mu$m, satur. level 0.25 pC/μm^2
- YAG screen has been applied for vacuum dependence and RF voltage dependence of vertical beam halo

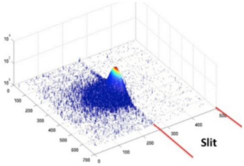

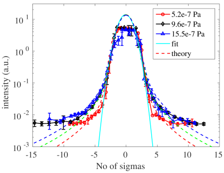

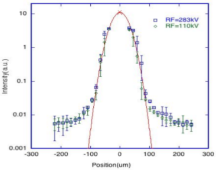

[1] T. Naito, IBIC15,TUPB024 (2015)

Upgrading for vertical & horizontal halo measurement

- Motivation: fast diagnostic of beam halo at dispersion free region
- Idea: 3 screens(2 YAG screens for halo and 1 OTR screens for beam core) are set to one holder high dynamic range 2D profile imaging

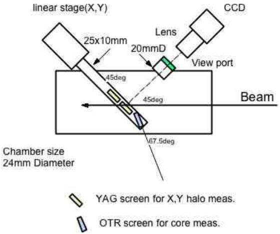

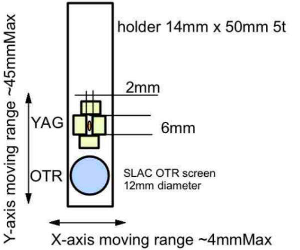

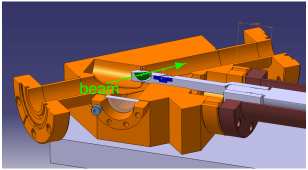

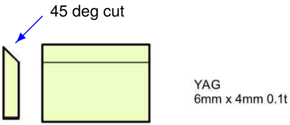

- Horizontal slices are cut by 45 deg to avoid edge effects (horizontal insert)

Improvement of motion system

- The RHUL-LW manipulator will be used (A. Aryshev and ATF team)

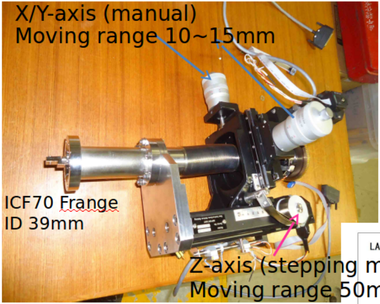

- *Manual micrometers have to be replaced by stepping motors*
- *Fortunately , used stepping motors could be applied (with new couples to connect motor and shaft)*
- *Four manipulator axes will be driven by the EPICS-compatible motion controller*

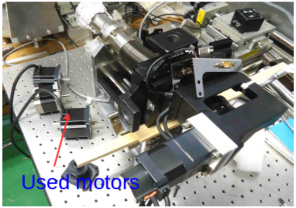

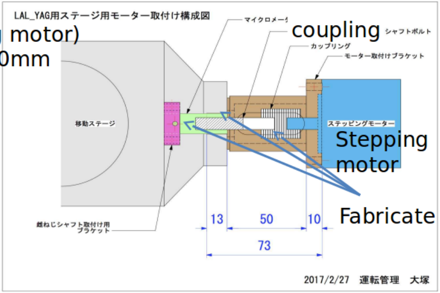

Wakefield property of OTR/YAG monitor

- Benchmarking based upon Ref. cavity (thanks to A. Lyapin)
- Simulation of wakefield with a simplified chamber/holder model
- Simulation parameter: $\sigma_z = 7$ mm, $Q = 1$ pC

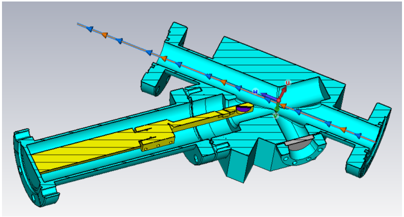

- $A_{wy} \approx 0.05$ V/pC and $A_{wx} \approx 0.4$ V/pC, with beam is displaced by 5 mm

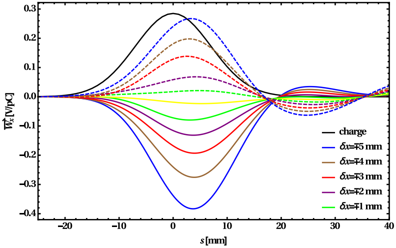

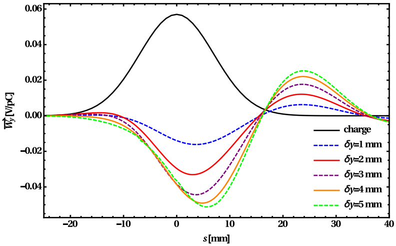

Effect of WK at YAG monitor to nanometer beam size

- Orbit change and beam size growth at IP can be estimated by linear calculation

$$\Delta y \approx R_{34} \frac{edy}{E} \int_{-\infty}^{\infty} W_T(z)\rho(z)dz$$

$$\Delta \sigma_y \approx \sqrt{R_{34}^2 (\frac{edy}{E})\sigma_w^2}$$

- Assuming beam offset 3 mm at YAG and beam intensity as 3×10^9/pulse
- Effects: $\Delta y = 0.9$ nm, $\Delta\sigma_y = 0.5$ nm; $\Delta x = 0.87$ μm, $\Delta\sigma_x = 0.02$ μm

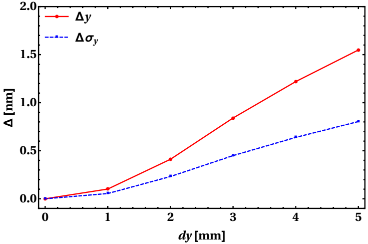

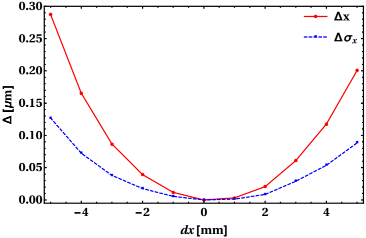

Expected performation and applications

- Resolution: OTR (from SLAC): 5∼10 μm , Ce:YAG: less than 10 μm
- Dynamic range: $< 10^4$ with present CCD , and hope to reach 10^5 with Hamamatsu 5985 CCD (sensitivity improved by 10^3)
- Application: Vacuum dependence, variation with extraction time for BGS halo and momentum diffusion study

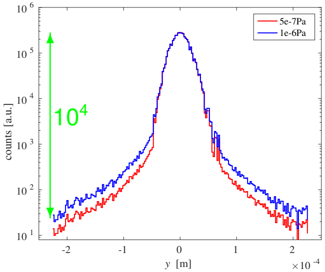

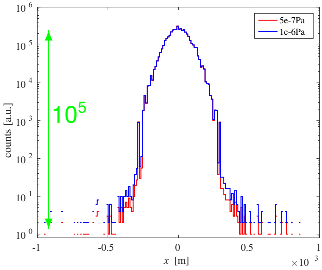

[1] M. Ross et al., SLAC-PUB-9280(2002)

[2] T. Naito, IBIC14,TUPD08 (2014)

Conclusion

- Simulation of BGS halo in damping ring indicate
  - Equilibrium halo distribution is mainly determined by BGS events within last 2τ
  - Good agreements are observed between simulation and theoretic estimation of beam halo
  - Simulation and theory both predict much less halo in $\vec{x}$ than $\vec{y}$
- With rescaling of DS data, vertical beam halo (vacuum dependence) are observed and consistent with theoretical prediction
- For halo study at dispersion-free region, upgrading of OTR/YAG screens monitor is underway (plan to install in May)
- Meanwhile, simulation of tail/halo from IBS (in SAD) is going on

Many thanks to for ATF collaboration!

Thank you for your attention!

Back up...

Simulation of vacuum lifetime

- Assuming BGS only includes elastic Coulomb scattering and Brems., tracking study based on the nominal parameter of DR

E (GeV)	P (Pa)	$\bar{\beta}_x/\bar{\beta}_y$ (m)	$\beta_{x,m}/\beta_{y,m}$ (m)	b_x/b_y (mm)	δ_{acc}
1.3	1×10^{-6}	4/4.6	22.5/23.4	7.5/12	0.01
ϵ_x (pm)	ϵ_y (nm)	σ_p	τ_{Coul} (min)	τ_{Brem} (min)	τ_v (min)
13.7	12	5×10^{-4}	101	341	78

- τ_v corresponds to transverse acceptance $\epsilon_A = 2\times10^{-6}$ (physical aperture)

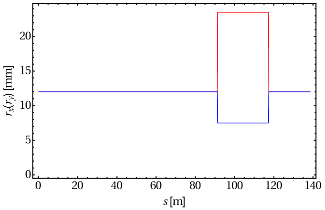

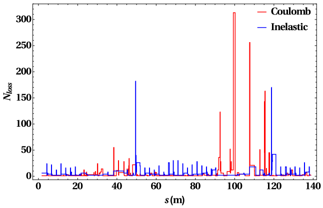

- More loss at the western arc section (min. A/β), especially region around the 1*nd* quad. entering the arc section (QM22R.1, QM22R.2)

Vacuum lifetime experiment in Jan. 2017

- Vertical emittance is variated by tuning SF1R magnet
- Two vacuum levels are considered ($2.3\times10^{-7}/1\times10^{-6}$ Pa)
- Bunch volume (σ_s,σ_p,ϵ_x and ϵ_y) evolution with beam intensity is included in analysis
- Current dependence of σ_s,σ_p,ϵ_x due to IBS is calculated by SAD
- ϵ_y is determined by $x-y$ coupling

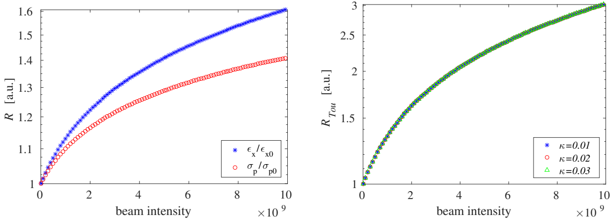

Vacuum lifetime experiment in Jan. 2017

- α and τ_{Tou} measured are different for variate vacuums
- $P \approx 2.3 \times 10^{-7}$ Pa: $\alpha \in [1000,1500]$ Pa^{-1}s^{-1}, τ_{Tou} ≈400/370 s

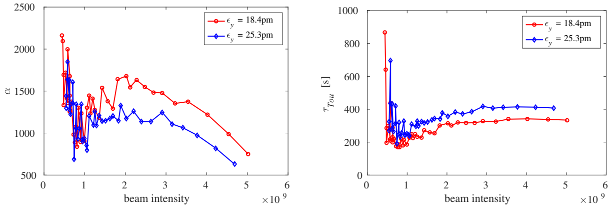

- $P \approx 1 \times 10^{-6}$ Pa: $\alpha \in [1000,1200]$ Pa^{-1}s^{-1}, τ_{Tou} ≈400/300 s

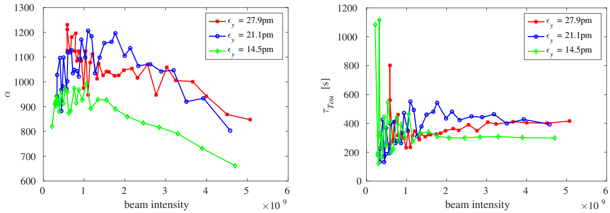

Halo evolution with storage time

- Theoretic estimation uses equilibrium σ_x or σ_y. Will it work well for beam in damping process ?
- Simulation of halo distribution at 120 ms, 150 ms and 200 ms

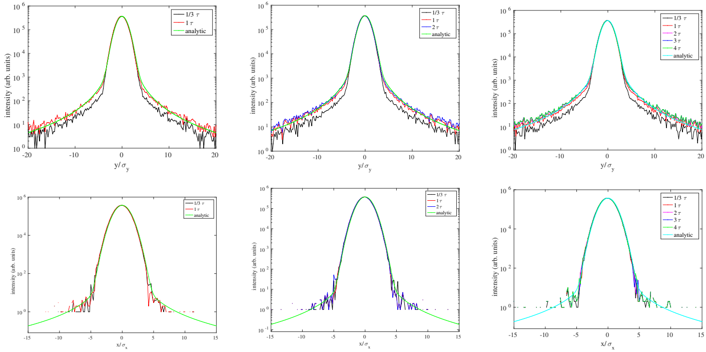

- ► Theoretic prediction still agrees well with tracking result ($t_n > 1, 2\tau_y$)
- ► Similar halo distribution when extract beam at different moment ?

Mechanism design of YAG/OTR chamber and holder

- Bellow at the holder pipe enables angle adjustment
- Indium seal is used for view window

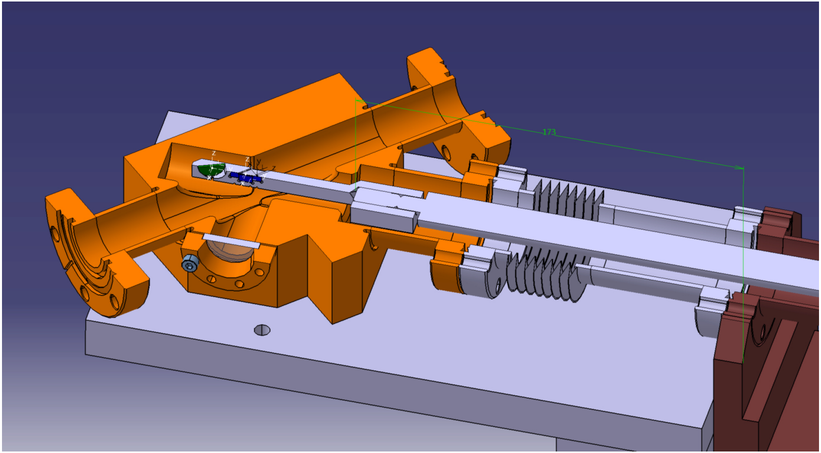

Mechanism design of YAG/OTR chamber and holder

- YAG pads and OTR screen are fixed by staples

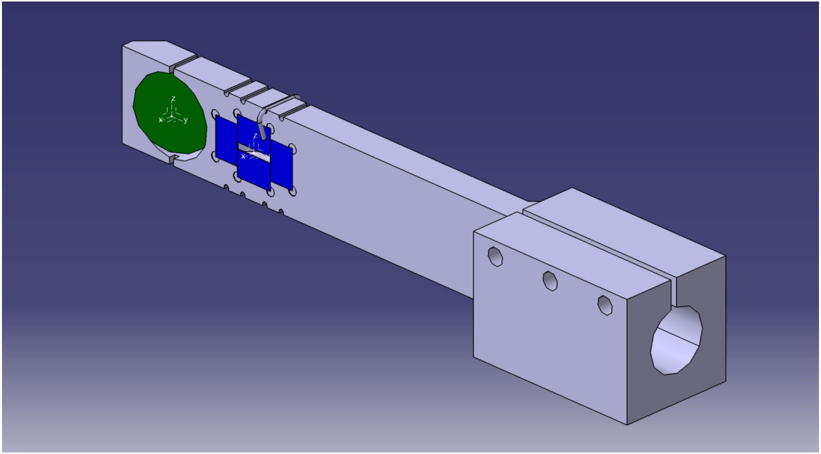

Benchmark of CST wakefield simulation

- Pill-box cavity of $\phi = 38.14$ mm, $l = 10$ mm and aperture of beam pipe is 16 mm

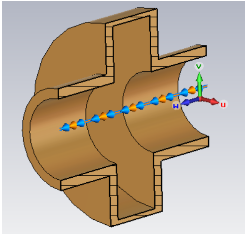

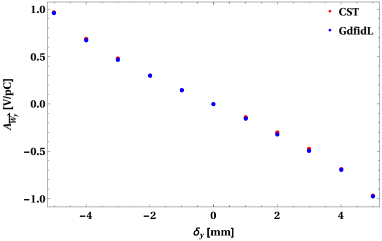

Comparison for 2 pipe types

- Wakefield and its effect of beam at IP are compared for $\phi 24 + \phi 40$ design and previous $\phi 24$ structure

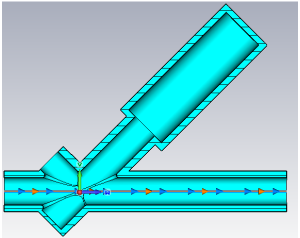

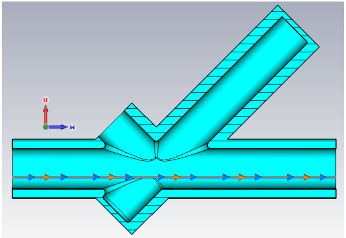

Comparison for 2 pipe types

- Similar A_{w_y} and A_{w_x} for previous and newest chamber structures

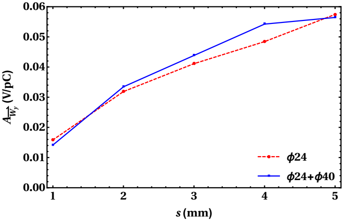

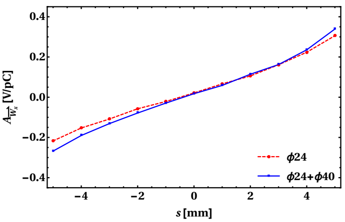

- Orbit and beam size distortions at IP didn't make obvious difference for two structures, vertically and horizontally

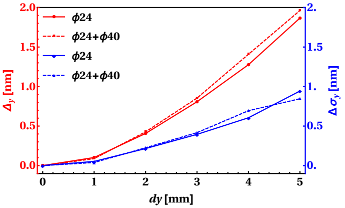

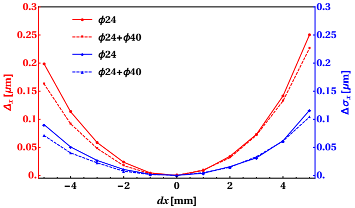

BGS halo study wit OTR/YAG

- BGS halo at YAG is simulated based BGS data in damping ring, and required $d_R \sim 10^6$
- Vacuum dependence and variation with extraction time for BGS halo are proposed to be measured by OTR/YAG

◦ Constant halo level and halo is expected for extraction at 150 ms and 200 ms

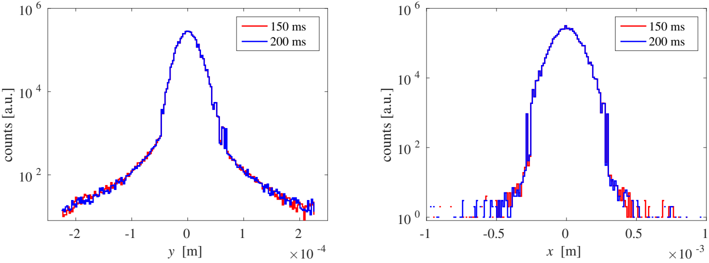

Momentum diffusion study at YAG

- Goal: diagnostic of dp/σ_p with higher d_R for halo study
- Fast measurement with large d_R ($\approx 10^6$)

- Tuning QF3X and QF4X to variate η_x and $\eta_{x'}$ at YAG
  - E.g. η_x=1.15 m and $\eta_{x'} = 0.385$ rad at YAG by varying K_1 of QF3X/QF4X

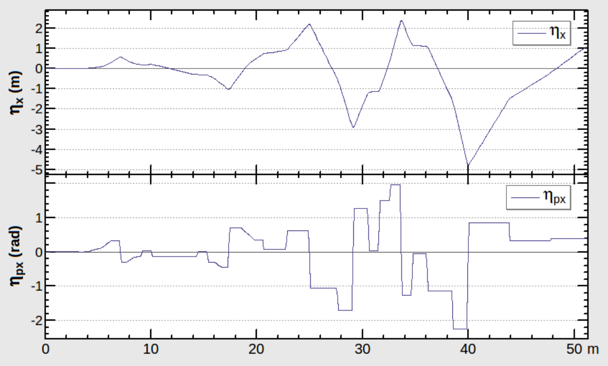

Momentum diffusion study at YAG

- Goal: diagnostic of dp/σ_p with higher d_R for halo study
- Fast measurement with large d_R ($\approx 10^6$) $\Rightarrow$ visualization of momentum diffusion (tail)
- Tuning QF3X and QF4X to variate η_x and $\eta_{x'}$ at YAG
  - E.g. η_x=1.15 m and $\eta_{x'} = 0.385$ rad at YAG by varying K_1 of QF3X/QF4X

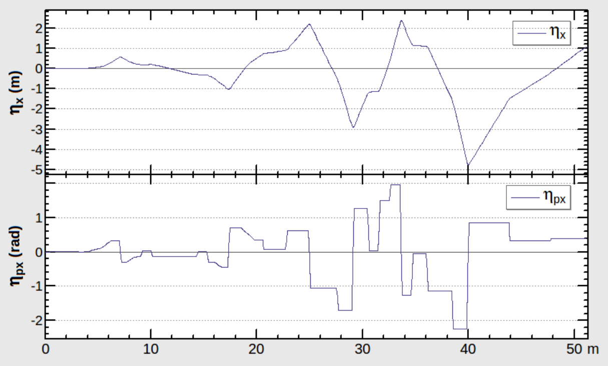

Momentum diffusion study at YAG

- Goal: diagnostic of dp/σ_p with higher d_R for halo study
- Fast measurement and $d_R \approx 10^6 \Rightarrow$ visualization of momentum diffusion (tail)
- Tuning QF3X and QF4X to variate η_x and $\eta_{x'}$ at YAG
- Assuming momentum has Gaussian core + exponent tail ($(dp/\sigma_p)^{-2}$), macro-particle tracking indicates the feasibility of fast imaging of dp/σ_p
  - η_x=1.15 m and $\eta_{x'} = 0.385$ rad at YAG by varying K_1 of QF3X/QF4X

Horizontal profile at YAG

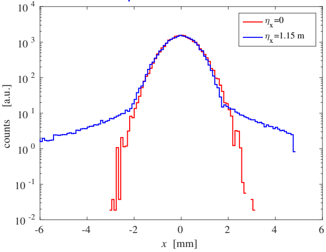

Horizontal profile VS. momentum spread